

Are your MRI contrast agents cost-effective?

Learn more about generic Gadolinium-Based Contrast Agents.



FRESENIUS
KABI

caring for life

AJNR

Are Gadolinium-Enhanced MR Sequences Needed in Simultaneous ^{18}F -FDG-PET/MRI for Tumor Delineation in Head and Neck Cancer?

N. Pyatigorskaya, R. De Laroche, G. Bera, A. Giron, C. Bertolus, G. Herve, E. Chambenois, S. Bergeret, D. Dormont, M. Amor-Sahli and A. Kas

This information is current as of April 17, 2024.

AJNR Am J Neuroradiol published online 24 September 2020

<http://www.ajnr.org/content/early/2020/09/24/ajnr.A6764>

Are Gadolinium-Enhanced MR Sequences Needed in Simultaneous ^{18}F -FDG-PET/MRI for Tumor Delineation in Head and Neck Cancer?

 N. Pyatigorskaya,  R. De Laroche,  G. Bera,  A. Giron,  C. Bertolus,  G. Herve,  E. Chambenois,  S. Bergeret,  D. Dormont,  M. Amor-Sahli, and  A. Kas



ABSTRACT

BACKGROUND AND PURPOSE: PET/MRI with ^{18}F -FDG has demonstrated the advantages of simultaneous PET and MR imaging in head and neck cancer imaging. MRI allowing excellent soft-tissue contrast, while PET provides metabolic information. The aim of this study was to evaluate the added value of gadolinium contrast-enhanced sequences in the tumor delineation of head and neck cancers on ^{18}F -FDG-PET/MR imaging.

MATERIALS AND METHODS: Consecutive patients who underwent simultaneous head and neck ^{18}F -FDG-PET/MR imaging staging or restaging followed by surgery were retrospectively included. Local tumor invasion and lymph node extension were assessed in 45 head and neck anatomic regions using ^{18}F -FDG-PET/MR imaging by 2 rater groups (each one including a radiologist and a nuclear medicine physician). Two reading sessions were performed, one without contrast-enhanced sequences (using only T1WI, T2WI, and PET images) and a second with additional T1WI postcontrast sequences. The results were compared with the detailed histopathologic analysis, used as reference standard. The κ concordance coefficient between the reading sessions and sensitivity and specificity for each region were calculated.

RESULTS: Thirty patients were included. There was excellent agreement between the contrast-free and postgadolinium reading sessions in delineating precise tumor extension in the 45 anatomic regions studied (Cohen $\kappa = 0.96$, 95% CI = [0.94–0.97], $P < .001$). The diagnostic accuracy did not differ between contrast-free and postgadolinium reading sessions, being 0.97 for both groups and both reading sessions. For the 2 rater groups, there was good sensitivity for both contrast-free (0.83 and 0.85) and postgadolinium reading sessions (0.88 and 0.90, respectively). Moreover, there was excellent specificity (0.98) for both groups and reading sessions.

CONCLUSIONS: Gadolinium chelate contrast administration showed no added value for accurate characterization of head and neck primary tumor extension and could possibly be avoided in the PET/MR imaging head and neck workflow.

ABBREVIATIONS: HNC = head and neck cancer; IDEAL = iterative decomposition of water and fat with least-square estimation; SUV_{max} = maximum standardized uptake value; PNS = perineural spread

Integrated PET/MR imaging systems are increasingly used in clinical practice. PET/MR imaging with ^{18}F -FDG has demonstrated the advantages of simultaneous PET and MR imaging, with MR imaging allowing excellent soft tissue contrast and PET providing metabolic information.^{1,2} This multimodality imaging may improve the diagnostic accuracy in complex anatomic regions.

Head and neck cancer (HNC) is a frequent pathology with high morbidity and mortality rates.³ Precise clinical and imaging


delineation of tumor expansion is challenging in the complex head and neck anatomic area. Nevertheless, accurate tumor delineation by imaging is essential for therapeutic decision making and for performing complete tumor resection while preserving healthy functional surrounding tissue.


In simultaneously acquired PET/MR imaging, MR images are the most time-consuming. PET/MR imaging in a clinical setting should be time-efficient for maintaining sufficient patient workflow and because the increase in acquisition time is a source of

Received July 10, 2019; accepted after revision June 21, 2020.

From Assistance Publique Hôpitaux de Paris Neuroradiology Department (N.P., E.C., D.D., M.A.-S.), and Nuclear Medicine Department (G.B., S.B., A.K.), Pitié-Salpêtrière-Charles Foix Hospital, Paris, France; Sorbonne University (N.P., D.D.), Pierre and Marie Faculty of Medicine, Paris, France; Nuclear Medicine Department (R.D.L.), Morvan Hospital, Brest, France; Sorbonne University (A.G., A.K.), Laboratoire d'Imagerie Biomédicale, Paris, France; Sorbonne University, Maxillo-Facial Surgery Department (C.B.), and Pathology Department (G.H.), Pitié Salpêtrière-Charles Foix Hospital, Assistance Publique Hôpitaux de Paris, Paris, France; and CIMI Sorbonne University UPMC (C.B.), Paris, France.

Please address correspondence to Nadya Pyatigorskaya, Service de Neuroradiologie, Hôpital Pitié-Salpêtrière, 47-83 Boulevard de l'Hôpital, 75651 Paris Cedex 13, France, e-mail: nadya.pyatigorskaya@gmail.com

 Indicates article with supplemental on-line table.

 Indicates article with supplemental on-line photos.

<http://dx.doi.org/10.3174/ajnr.A6764>

motion artifacts and patient discomfort. Still, protocol optimization should not lead to the degradation of imaging quality and diagnostic accuracy. PET/MR imaging acquisition commonly includes a head and neck MR imaging protocol usually performed in clinical practice^{4,5} and PET acquisition. However, in clinical context, each MR image should provide additional information to that provided by ¹⁸F-FDG-PET. Consequently, the utility of each MR image in this combined examination should be questioned and justified.

Gadolinium contrast-enhanced sequences are useful in the detection and delineation of head and neck tumors.⁶ However, these sequences are time-consuming, and gadolinium administration can cause potential side effects such as nephrogenic systemic sclerosis^{7,8} or gadolinium chelate brain accumulation.⁹

Thus, before including a contrast-enhanced MR image in the protocol of simultaneous PET/MR imaging for head and neck examination, it is important to first examine whether gadolinium-enhanced sequences provide any additional information of value compared with ¹⁸F-FDG-PET/MR imaging including only nonenhanced morphologic MR images.¹⁰ Indeed, although gadolinium contrast-enhanced sequences are known to have an important place in MR imaging examination, there is currently no evidence concerning their usefulness in simultaneous head and neck ¹⁸F-FDG-PET/MR imaging acquisition.¹¹ Only 1 study on a pediatric population investigated whether gadolinium contrast enhancement added any information in PET/MR imaging, finding no notable difference in the diagnostic accuracy between the enhanced and unenhanced images.¹² Another study, which investigated the added value of MR imaging sequences compared with PET/CT, suggested that PET/MR imaging could be a legitimate alternative to PET/CT in patients with HNC.¹¹ To the best of our knowledge, no study has yet systematically investigated whether gadolinium contrast-enhanced sequences provide any additional information compared with contrast-free simultaneous ¹⁸F-FDG-PET/MR imaging for assessing precise local and regional invasion in HNC.

The aim of this study was to evaluate the added value of gadolinium contrast-enhanced sequences for HNC tumor delineation using ¹⁸F-FDG-PET/MR imaging to examine the usefulness of this sequence in HNC PET/MR imaging protocols.

MATERIALS AND METHODS

Patients

Thirty consecutive patients with histopathologically confirmed HNC examined in our institution between November 2015 and June 2016 were retrospectively included. The inclusion criteria were available simultaneous ¹⁸F-FDG-PET/MR imaging scan performed in the context of staging or restaging the histopathologically confirmed HNC, which included the sequences with and without contrast administration, and head and neck surgery performed within 4 weeks after the PET/MR imaging examination with available detailed pathologic analysis of precise tumor extension. None of the patients were undergoing any therapy at the time of imaging or in the interval between the imaging and the resection. The restaging examination was performed at least 4 weeks after the surgery and 12 weeks after radiation therapy, as previously recommended for posttreatment evaluation in HNC.^{13,14}

The data for this study were extracted from the local data base of PET/MR imaging examinations, which was approved by the French authority for the protection of privacy and personal data in clinical research (CNIL, approval No. 2111722). This study was performed according to the principles of the Declaration of Helsinki.

Imaging Protocol

All the images were acquired simultaneously with an integrated PET/MR imaging system (Signa 3T, GE Healthcare) using the same protocol, 60 minutes after IV injection of 3.7 MBq/kg ¹⁸F-FDG. No patients had blood glucose level >11 mmol/L, and all had been fasting for 6 hours or more before the ¹⁸F-FDG injection. Contraindications for MR imaging were respected.

Simultaneous PET/MR imaging acquisition was performed in the head and neck region using a 40-channel head and neck receiver coil; the duration time was approximately 20 min. The protocol included a 2-point Dixon MR imaging sequence for the attenuation correction (which resulted in in-phase T1WI, out-of-phase T1WI, water-only, and fat-only images); an axial FSE T1WI, iterative decomposition of water and fat with least-square estimation (IDEAL) FSE axial T2WI sequence; and a 3D contrast-enhanced FSE T1WI acquired immediately after the injection of gadoterate meglumine (Dotarem 0.2 mL/kg, Guerbet). The simultaneous PET acquisition, which lasted 16 minutes, was followed by a whole-body simultaneous PET/MR imaging acquisition from the neck to the proximal femur, including 4 bed-PET/MR imaging position scans. Finally, an axial postcontrast-injection IDEAL FSE T1WI, a coronal IDEAL FSE T2WI, and an axial DWI centered on the head and neck region were acquired during about 8 minutes. The total duration of PET/MR imaging examination was 45–50 minutes.

PET data were reconstructed iteratively using the ordered subsets expectation maximization algorithm, integrating TOF, point spread function modeling, and attenuation, truncation, and scatter corrections with a matrix size of 256 × 256, 4 iterations and 28 subsets, and a filter cutoff of 3 mm for head and neck scans, resulting in voxel size of 1.17 × 1.17 × 2.78 mm. For photon attenuation correction, a 2-point Dixon MR imaging was used.

Image Analysis

PET/MR images were analyzed by 2 rater groups, each comprising an experienced radiologist (M.A.-S. or N.P.) and an experienced nuclear medicine physician (A.K. or G.B.) with at least 11 years of practice. The raters performing the PET/MR imaging readings were blinded to previous medical history, suspected diagnosis, pathologic findings, and other imaging technique results. Whole-body PET/MR imaging and DWI were unavailable to the raters during the reading. The images were analyzed using an Advantage Workstation 4.6 (AW4.6, GE Healthcare).

For the first reading session (referred to as “contrast free”), only PET images and contrast-free spin-echo T1WI and IDEAL T2WI were available for simultaneous interpretation. For each of the 45 specific anatomic regions

Table 1: Lesion characteristics

	Total Number of Subjects (%)	Number of Subjects with T1–T2 Lesions (%)
Histologic type		
Squamous cell carcinoma	23 (77%)	8 (80%)
Adenoid cystic carcinoma	4 (13%)	1 (10%)
Adenocarcinoma	1 (3%)	1 (10%)
Sarcoma	1 (3%)	
Melanoma metastasis	1 (3%)	
Tumor stage		
pT1	4 (13%)	4 (40%)
pT2	6 (20%)	6 (60%)
pT3	1 (3%)	
pT4	16 (53%)	
Lymph node stage		
pN0	12 (38%)	
pN1	5 (17%)	
pN2a	1 (3%)	
pN2b	6 (20%)	
pN2c	1 (3%)	
pN3	0	
Initial tumor location		
Base of tongue	1 (3%)	
Tongue	6 (20%)	2 (20%)
Floor of mouth	4 (13%)	3 (30%)
Vestibule or lip	2 (7%)	
Maxillary	2 (7%)	
Palate	3 (10%)	
Mandibular	8 (27%)	
Amygdala	1 (3%)	3 (30%)
Salivary glands	3 (10%)	2 (20%)
Staging		
Initial diagnosis	23 (77%)	6 (60%)
Recurrence	7 (23%)	4 (40%)

determined together with the pathologists (On-line Table), the raters had to specify the presence or absence of tumor invasion. All areas of focal uptake were identified and correlated to the corresponding MR images. Analyses of the PET/MR imaging data included qualitative and quantitative assessment. Areas of focal ¹⁸F-FDG-uptakes were classified as probably malignant or as probably benign based on visual analysis, focused on the pattern and asymmetry of FDG distribution as well as contrast to background uptake, especially in anatomic structures with physiologic uptake (eg, palatine tonsils or salivary glands). The semiquantitative standardized uptake value (SUV_{max}) was used as a tool to supplement visual interpretation. SUV_{max} values were measured in tissues or nodes with increased ¹⁸F-FDG uptake using a volume of interest based on a 40% isocontour threshold with an AW4.6 workstation.^{15,16} The morphologic criteria for tumor malignancy included a masslike lesion with irregular borders, low T1-weighted signal, and usually iso or high T2-weighted signal. The combination of the most relevant findings (morphologic and metabolic) was considered for the PET/MR imaging classification. The lesions were classified by consensus using a qualitative 2-point scale as follows: 1 represented malignant tumor invasion of the anatomic region, and 0 represented the absence of suspicious invasion. The same reading was performed for

the assessment of lymph node involvement. Lymph nodes with suspected malignant invasion were reported in each anatomic region. The size, shape, homogeneity, capsular disruption, and intensity of ¹⁸F-FDG uptake were taken into consideration.

The second interpretation session (referred to as “postgadolinium”) followed the same method of analysis, which additionally included gadolinium-enhanced images and the assessment of contrast enhancement in each region. The time interval between the 2 reading sessions was at least 8 weeks.

Histopathologic Analysis

All the lesions were analyzed by an experienced senior anatomopathologist with 14 years of experience (G.H.). Each of the included patients had a histopathologic confirmation of the lesion nature. Histopathologic tumor grade, surgical margin invasion by the tumor, and invasion of each of the 45 systematically examined anatomic regions (On-line Table) were determined. The histopathologic results were considered as standard of reference for this study. Only lymph nodes with available pathology analysis were considered.

Only lymph nodes with available pathology analysis were considered.

Statistical Analysis

Statistical analysis was performed using JMP Pro 14 (SAS Institute). The interrater agreement and the agreement between contrast-free and postgadolinium sessions were estimated using the Cohen κ coefficient for each region and for each reading session. The sensitivity, specificity, and diagnostic accuracy were also calculated for each region for each reading session. Additionally, the overall diagnostic accuracy was estimated. The values between 0.9 and 1 were considered “excellent,” between 0.80 and 0.90 as “good,” and between 0.70 and 0.80 as “fair.” These values were also determined for a subgroup analysis ($n = 10$) of small-sized tumors (stage T1 and T2 according to the American Joint Committee on Cancer *Cancer Staging Manual* 7th edition, being applicable at the time of the study) because these lesions are considered to be more difficult to detect and explore.¹⁷

RESULTS

Patients and Lesions

Thirty consecutive patients (61.6 ± 16.8 years old, 12 women) were retrospectively included. Histopathologic tumor types included squamous cell carcinomas ($n = 23$), adenoid cystic

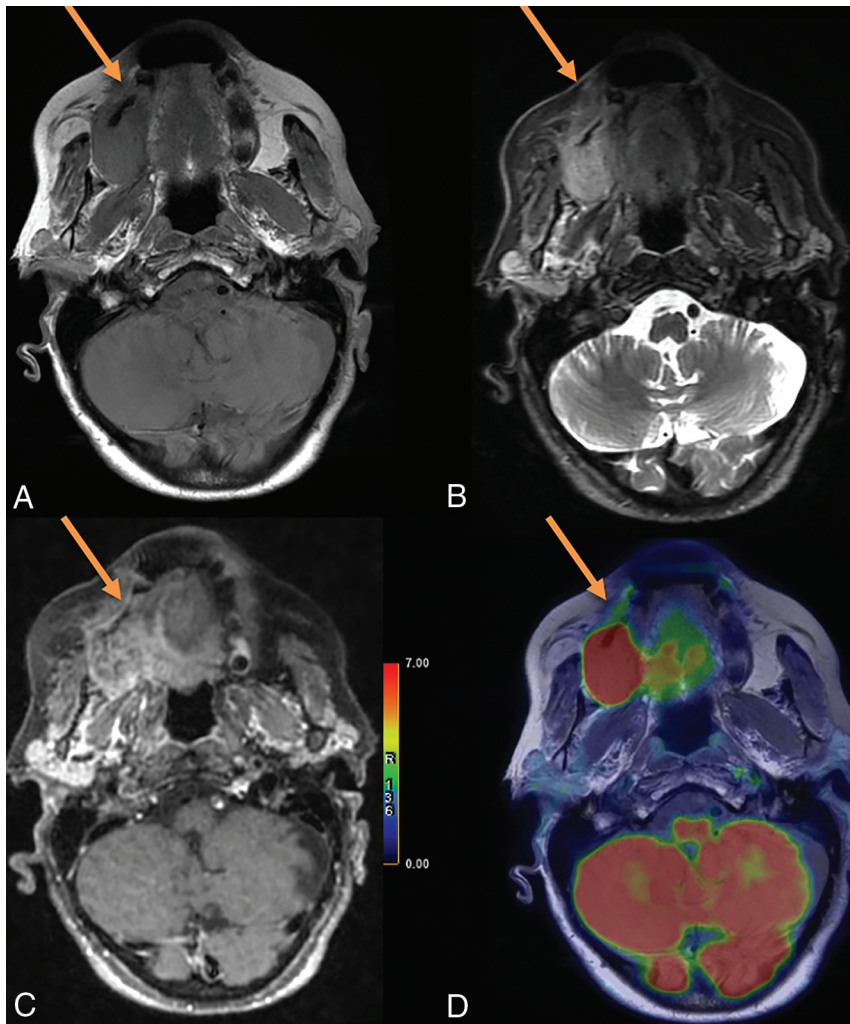


FIG 1. Initial staging of a right maxillary squamous cell carcinoma in an 84-year-old woman. A, Axial T1-weighted spin-echo (SE) sequence. B, Axial T1-weighted fat-saturated sequence. C, Fusion between axial T1-weighted SE sequence. C, 3D T1-weighted fat-saturated SE postcontrast sequence, axial plane. D, Fusion between axial T1-weighted SE sequence and ^{18}F -FDG-PET. Both T1-weighted FDG-PET/MR imaging with and without gadolinium showed right hard palate invasion. The anterior tumor margin (*arrow*) was difficult to define on both contrast-free and postcontrast T1WI (B and D). PET imaging allowed clarification of the lesion margins (A and C).

carcinomas ($n = 4$), adenocarcinoma ($n = 1$), sarcoma ($n = 1$), and melanoma metastasis ($n = 1$). Twenty-five patients (83%) underwent cervical lymph node resection; in 19 (76%) patients, the resection was unilateral, and in 6 (24%) patients, it was bilateral. A total of 142 cervical lymph nodes were analyzed. The head and neck surgery was performed within 25.8 ± 13.2 (range, 2–29) days after the PET/MR imaging examination. The lesion characteristics are shown in Table 1, Figs 1–3, and On-line Figs 1 and 2.

Agreement between Evaluations

There was excellent agreement between the contrast-free and postgadolinium reading sessions for the precise assessment of tumor extension (Cohen $\kappa = 0.96$, 95% CI = [0.94–0.97], $P < .001$). Good interrater agreement was also found for the contrast-free session ($\kappa = 0.78$, 95% CI = [0.74–0.81], $P < .001$) and for the

postgadolinium session ($\kappa = 0.78$, 95% CI = [0.73–0.83], $P < .001$). The data for each region are detailed in the On-line Table.

Diagnostic Accuracy

The diagnostic accuracy did not differ between the contrast-free and postgadolinium reading sessions (0.97 for both groups and both reading sessions). For the first group (A.K. and M.A.-S.), there was good sensitivity for both contrast-free and postgadolinium reading sessions (0.83 and 0.85, respectively), and there was excellent specificity (0.98 for each reading session). For the second raters group (G.B. and N. P.), there was also good sensitivity (0.88 and 0.9, respectively), and there was excellent specificity (0.98 for each reading session). The data regarding the sensitivity and specificity for the assessment of tumor invasion for each of the 45 anatomic regions are detailed in Table 2.

Lymph Node Analysis

The agreement between the contrast-free and postgadolinium sessions was good (Cohen $\kappa = 0.90$, 95% CI = [0.78–0.95], $P < .001$). For both contrast-free and postgadolinium reading sessions, there was good sensitivity (0.85), and there was excellent specificity (0.97 and 0.98, respectively).

Subgroup Analysis

For small-sized tumor lesions (T1–T2 stages), there was also excellent intrarater agreement for tumor extension assessment between the contrast-free and postgadolinium reading sessions

(Cohen $\kappa = 0.91$, 95% CI = [0.85–0.96], $P < .001$). The diagnostic accuracy for T1–T2 lesions did not differ from the overall accuracy (0.97 for both groups and both reading sessions). For the first rater group, there was good sensitivity (0.79 for both contrast-free and postgadolinium sessions), and there was excellent specificity (0.98 for both reading sessions). For the second rater group, the sensitivity was good (0.89 and 0.79, respectively), and specificity was excellent (0.99 for both reading sessions).

DISCUSSION

We observed excellent diagnostic accuracy of simultaneous ^{18}F -FDG-PET/MR imaging for the assessment of locoregional extension of HNC with or without gadolinium contrast administration. There was excellent agreement between the contrast-free and postgadolinium reading sessions, and there were good sensitivity and

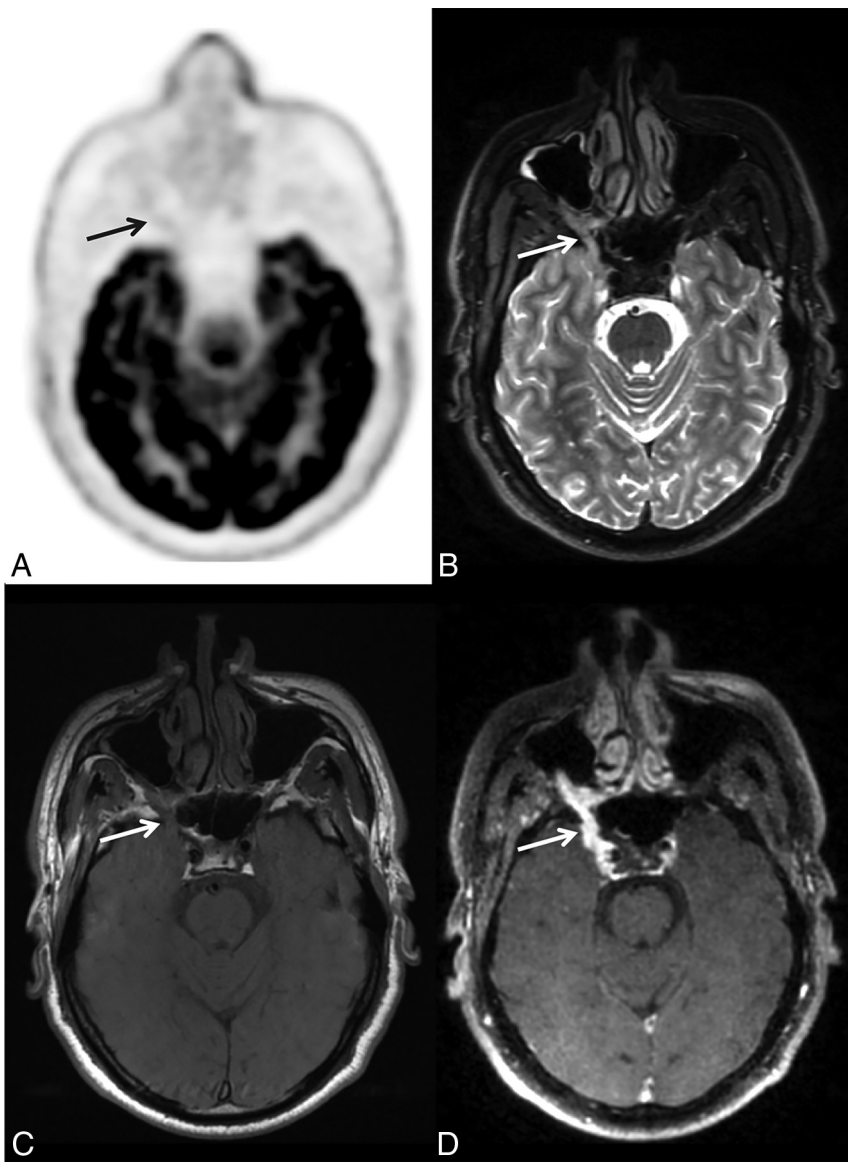


FIG 2. Initial staging of right adenoid cystic carcinoma of a minor salivary gland (palate) in a 55-year-old man. *A*, Axial FDG-PET. *B*, Axial T2-weighted spin-echo (SE) sequence. *C*, Axial T1-weighted SE sequence. *D*, 3D T1-weighted fat-saturated SE postcontrast sequence. On both T1-weighted and T2-weighted MR imaging (*B* and *C*), thickening of the trigeminal nerve is present, with a loss of signal of the fatty tissue in the pterygopalatine fossa, strongly suggestive of perineural spread of the tumor. On the T1-weighted postgadolinium sequence (*D*), high enhancement of the trigeminal nerve is visible (arrow). There is no significant perineural ^{18}F -FDG uptake (*A*); only slight uptake is discernible when guided by MR imaging findings.

excellent specificity for the assessment of local tumor extension as well as for the evaluation of lymph node involvement, similarly with and without gadolinium injection.

To the best of our knowledge, this is the first simultaneous PET/MR imaging study investigating the added value of gadolinium-enhanced sequences in adults and the first study of the head and neck region.

To this day, several studies have debated on the added value of PET/MR imaging compared with PET/CT in HNC evaluation. Although some studies found no advantages of PET/MR imaging

in terms of diagnostic performance,^{16,18-20} others showed it to be advantageous in terms of overall diagnostic accuracy²¹ or of tumor delineation,²² which is particularly relevant in the head and neck region, where anatomic landmarks are complex and mobile because of patients positioning differences between examinations.²³ Additionally, coregistration procedures between PET/CT and MR imaging are usually performed in studies conducted for research purposes, being less feasible in clinical practice using routine algorithms. Consequently, several studies have demonstrated the superiority of PET/MR imaging versus PET/CT²⁴ and versus the association of PET/CT and MR imaging.^{25,26}

The main drawback of PET/MR imaging is its long acquisition time.²⁷ However, although the duration of PET/MR imaging is longer than that of PET/CT, it should be pointed out that acquiring simultaneous PET/MR imaging data reduces the overall examination time compared with sequential PET/CT and MR examinations. PET/MR imaging should still be as short as possible for clinical workflow optimization, especially in patients with HNC, who often have swallowing or breathing difficulties.

In PET/MR workflow considerations, the limiting factor for reducing the acquisition time is the MR imaging and not the PET acquisition. Indeed, transaxial PET data for a 25-cm fields of view are acquired within ≤ 10 min, whereas simultaneously acquired MR pulse sequences require much longer imaging times.

In the context of workflow optimization, one should question the relevance of each MR image. Furthermore, the information provided by PET and MR modalities should be as complementary as possible, any redundancy being avoided.

Avoiding contrast injection is also preferable in patients with severe renal failure, who are at risk of developing nephrogenic systemic sclerosis,^{7,8} especially in the case of repeated injections and if the linear-structured gadolinium-chelated molecules are used.²⁸ Moreover, gadolinium chelate deposition in the brain was recently reported,⁹ especially in patients undergoing repeated injections, as would be the case for

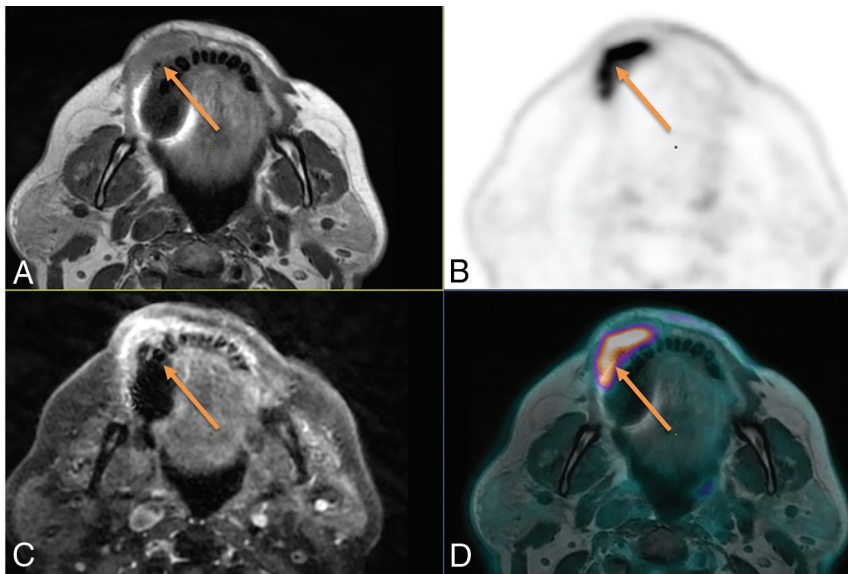


FIG 3. Local extension of a mandibular gingiva tumor in a 71-year-old woman. A, Axial contrast-free T1-weighted. B, Axial ^{18}F -FDG-PET image. C, 3D T1-weighted spin-echo (SE) contrast-enhanced sequence, axial plane. D, Fusion between axial T1-weighted and ^{18}F -FDG-PET. Both contrast-free and gadolinium-enhanced T1W MR imaging showed right vestibular invasion. Although bone invasion remained doubtful because of dental artifacts on MR alone, high FDG uptake includes a portion of the mandibular bone with margins that are clearly visible on the fusion images between PET and T1-weighted MRI, demonstrating bone involvement (arrow), which was pathologically confirmed.

certain patients with HNC with long follow-up times. Even though the clinical impact of these deposits remains unclear, there is a current trend of reducing the overall received dose of gadolinium, especially in patients with a good prognosis and a high life expectancy.

Although this is the first study directly investigating the value of gadolinium injection in HNC simultaneous PET/MR imaging protocols for precise assessment of tumor invasion, DWI has already been similarly examined^{22,29} with the results suggesting that it has no added value in the PET/MR imaging protocol.^{22,29} Indeed, significant correlation between DWI-ADC and SUV_{max} values on PET images was found.^{16,21,30,31} In contrast to this, in another study, it was observed that PET/MR-DWI may help to avoid false-positive findings caused by nonspecific FDG uptake in the case of tumor recurrence.²¹

Previously, it was reported that fat-suppressed contrast-enhanced T1-weighted MR images are superior to unenhanced ones for tumor diagnosis

Table 2: Diagnostic accuracy of contrast-free and postgadolinium sessions

	First Raters Group				Second Raters Group			
	Contrast-Free Session		Postgadolinium Session		Contrast-Free Session		Postgadolinium Session	
	Se	Sp	Se	Sp	Se	Sp	Se	Sp
Region extension								
Median line involvement	0.67	0.96	0.67	0.95	0.83	0.95	0.83	0.95
Vascular extension	0	1	0	1	1	0.93	1	0.93
Mandibular cortical bone	0.9	0.95	0.9	0.95	0.9	0.95	0.9	0.95
Mandibular medullary bone	0.88	0.9	0.88	0.9	0.88	0.9	0.88	0.9
Intermaxillary commissure	1	0.91	1	0.86	1	0.95	1	0.89
Vestibule	0.92	1	0.92	1	0.92	1	0.92	1
Skin	0.67	1	1	1	0.67	0.92	0.67	1
Mobile tongue	0.8	1	0.8	1	0.67	1	0.67	1
Palatoglossal arch	0.67	1	0.33	1	1	0.96	0.67	1
Palatine tonsil	1	0.92	1	0.92	1	1	0.5	1
Floor of mouth	0.78	0.94	0.78	0.94	0.89	1	0.89	1
Submandibular glands	1	0.9	1	0.9	1	1	1	1
Soft palate	0.67	0.96	0.67	1	1	0.81	1	0.81
Hard palate	1	1	1	1	1	0.96	1	0.96
Maxillary bone	1	0.96	1	0.96	1	0.92	1	0.92
Maxillary sinus	1	0.96	1	0.96	1	0.96	1	0.96
Masseter muscle	1	0.96	1	0.96	1	0.96	1	1
Pterygoid muscles	1	0.89	1	0.92	1	0.88	1	0.88
Nasal fossa	1	1	1	1	0.5	0.96	1	0.96
Subarachnoid spaces	1	1	1	1	1	1	1	1
Parotid glands	0	1	1	1	1	1	0	1
Perineural extension (V)	1	1	1	1	1	0.96	1	0.96
Perineural extension (VII)	0	1	0.5	1	1	1	1	1
All locations	0.83	0.98	0.85	0.98	0.88	0.98	0.9	0.98
All locations T1-T2	0.79	0.99	0.79	0.99	0.79	0.98	0.89	0.98

Note:—Se indicates sensitivity; Sp, specificity.

in the head and neck region.³² Contrast enhancement has shown an ability to improve lesion detection and tissue characterization and to facilitate the evaluation of tumor extension. However, some studies with advanced morphologic MR images, such as fast short inversion recovery MR imaging, have shown comparable results to postgadolinium sequences for soft tissue tumor characterization.³³

Whereas postgadolinium contrast enhancement reflects the tumor vascularization,³⁴ ¹⁸F-FDG reflects glucose metabolism.³⁵ Even if the pathophysiological mechanisms are different, our study suggests that contrast-free MR imaging morphologic sequences with simultaneous ¹⁸F-FDG PET images may give the same information as that added by postgadolinium sequences. In other words, the postgadolinium sequence does not seem to improve diagnostic accuracy in patients explored by simultaneous ¹⁸F-FDG-PET/MR imaging. On the basis of retrospectively fused PET/CT and MR imaging, Kuhn et al¹¹ previously suggested that gadolinium contrast enhancement gave added value to the evaluation of primary tumor extension compared with fused PET and T2-weighted images alone. However, in our study, using simultaneous PET/MR imaging, the diagnostic accuracy in the evaluation of precise tumor extension remains the same with or without post-contrast images, suggesting that gadolinium-enhanced MR images provide redundant information compared with simultaneously acquired nonenhanced morphologic MRI together with FDG-PET images.

Although several previous PET/MR imaging studies focused on its diagnostic performance in head and neck tumor detection,^{2,18,26} the present work, to the best of our knowledge, is the first study presenting a precise mapping of the regional HNC extension areas, analyzed by means of simultaneous PET/MR imaging. Previously, it was suggested that postcontrast T1-weighted sequences allow detection of perineural spread.¹¹ In our study, 1 rater group correctly detected all of the 3 cases of perineural spread on both contrast-free and postgadolinium sessions, but for the second rater group, detection was facilitated by contrast enhancement in 1 case. In the present study, thorough analysis of contrast-free simultaneous PET/MR imaging alone allowed detection of perineural spread in most cases. However, studies including larger numbers of cases of perineural spread are needed to corroborate this finding. Perineural spread (PNS) is a significant element of patient prognosis and long-term survival, and noncontrast MR imaging may be limited in this regard, but PET/CT has been widely applied in patients with multiple head and neck tumors at risk of having PNS, knowing the limitation of the study. At this stage, considering that PNS can be subtle with a non-negligible risk of omission and that postgadolinium MR clearly increases the radiologist's degree of confidence, postcontrast sequences should be maintained in ¹⁸F-FDG-PET/MR for salivary gland malignancy work-up (given the high propensity for nerve invasion³⁶) or when PNS is clinically suspected. Still, with the exception of those particular cases, our results suggest that analyzing contrast-free MR

imaging simultaneously with ¹⁸F-FDG PET in the context of PET/MR provides optimal diagnostic accuracy without the need for gadolinium-enhanced sequences.

Assessment of potential tumor invasion of bony structures, such as the mandible or maxillary sinus, has been reported as challenging, and some studies have suggested, in this case, better specificity and sensitivity of CT compared with MR imaging³⁷ or PET/MR imaging.¹¹ However, other studies found good diagnostic accuracy for both CT and MR imaging.³⁸ Moreover, higher confidence of PET/MR imaging compared with PET/CT for bone lesion detection has been reported.³⁹ In our study, all cases of mandibular bone cortical and medullary invasion were correctly detected in the contrast-free session alone, with 1 exception, in which even gadolinium injection did not facilitate the detection. Therefore, PET/MR imaging diagnostic accuracy for bone lesion detection appears to be good and does not seem to be improved by contrast enhancement.

Detection of small-sized head and neck tumors can be particularly challenging.⁴⁰ In this context, one could suppose that all available MR images should be used to maximize the chances of precise lesion detection and delineation. However, in the present study, we have observed that the diagnostic accuracy was good for both reading sessions with no improvement of sensitivity or specificity when a contrast-enhanced sequence was added.

PET/MR appears to be an advantageous imaging method in HNC because it can simultaneously evaluate the locoregional tumor extension, lymph node involvement, and distant metastases by combining head and neck MR imaging and whole-body ¹⁸F-FDG-PET, 2 imaging modalities recommended for HNC staging. Still, in our opinion, management of patients with HNC should also systematically include head and neck and chest CT in search of cortical bone erosion, enlargement of foramina, and lung nodules.

Our study has several limitations. First, the sample size was small in this proof-of-concept study. Still, despite this, the results appear to be significant and promising. Second, because of the clinical design of the study, there was heterogeneity concerning histopathologic tumor types, related to the local recruitment. However, the main lesions were large oral cavity squamous cell carcinoma and salivary gland adenoid cystic carcinoma, with all the detailed histologic data available. Different histologic types of tumors might be different in contrast enhancement and FDG uptake. Namely, we could expect that some adenoid cystic tumors may show important contrast enhancement with moderate hypermetabolism. Still, in our study, we have not observed added value of contrast enhancement for these tumors. In the future, it might be interesting to conduct larger scale studies focused on the adenoid cystic tumor subtype, which remains difficult because of the low prevalence of these tumors. Last, there were few cases of perineural spread, which is consistent with the rarity of adenoid cystic carcinoma and of perineural spread.

CONCLUSIONS

In our study, the diagnostic accuracy of simultaneously acquired PET/MR imaging for assessing locoregional extension in patients with HNC was comparable with or without the addition of a gadolinium-enhanced sequence. These results suggest that in the specific case of simultaneously acquired head and neck PET/MR imaging, contrast injection does not provide added value to HNC evaluation and may be avoided.

Disclosures: Nadya Pyatigorskaya—UNRELATED: Payment for Lectures Including Service on Speakers Bureaus: GE Healthcare. Aurelie Kas—UNRELATED: Payment for Lectures Including Service on Speakers Bureaus: Lecture in EANM session about clinical PET/MR imaging*; Payment for Development of Educational Presentations: PIRAMAL, Comments: Educational session for nuclear physicians about amyloid-PET imaging but without any influence on the current work.* *Money paid to institution.

REFERENCES

- Schaarschmidt BM, Heusch P, Buchbender C, et al. **Locoregional tumour evaluation of squamous cell carcinoma in the head and neck area: a comparison between MRI, PET/CT and integrated PET/MRI.** *Eur J Nucl Med Mol Imaging* 2016;43:92–102 [CrossRef Medline](#)
- Xiao Y, Chen Y, Shi Y, et al. **The value of fluorine-18 fluorodeoxyglucose PET/MRI in the diagnosis of head and neck carcinoma: a meta-analysis.** *Nucl Med Commun* 2015;36:312–18 [CrossRef Medline](#)
- Gupta B, Johnson NW, Kumar N. **Global epidemiology of head and neck cancers: a continuing challenge.** *Oncology* 2016;91:13–23 [CrossRef Medline](#)
- Widmann G, Henninger B, Kremser C, et al. **MRI sequences in head & neck radiology—state of the art.** *Rofo* 2017;189:413–22 [CrossRef Medline](#)
- Ozturk M, Yorulmaz I, Guney E, et al. **Masses of the tongue and floor of the mouth: findings on magnetic resonance imaging.** *Eur Radiol* 2000;10:1669–74 [CrossRef Medline](#)
- Ross MR, Schomer DF, Chappell P, et al. **MR imaging of head and neck tumors: comparison of T1-weighted contrast-enhanced fat-suppressed images with conventional T2-weighted and fast spin-echo T2-weighted images.** *Am J Roentgenol* 1994;163:173–78 [CrossRef Medline](#)
- Weller A, Barber JL, Olsen OE. **Gadolinium and nephrogenic systemic fibrosis: an update.** *Pediatr Nephrol* 2014;29:1927–37 [CrossRef Medline](#)
- Weinreb JC, Abu-Alfa AK. **Gadolinium-based contrast agents and nephrogenic systemic fibrosis: why did it happen and what have we learned?** *J Magn Reson Imaging* 2009;30:1236–39 [CrossRef Medline](#)
- McDonald RJ, McDonald JS, Kallmes DF, et al. **Intracranial gadolinium deposition after contrast-enhanced MR imaging.** *Radiology* 2015;275:772–82 [CrossRef Medline](#)
- von Schulthess GK, Veit-Haibach P. **Workflow considerations in PET/MR imaging.** *J Nucl Med* 2014;55:19S–24S [CrossRef Medline](#)
- Kuhn FP, Hüllner M, Mader CE, et al. **Contrast-enhanced PET/MR imaging versus contrast-enhanced PET/CT in head and neck cancer: how much MR information is needed?** *J Nucl Med* 2014;55:551–58 [CrossRef Medline](#)
- Klenk C, Gawande R, Tran VT, et al. **Progressing toward a cohesive pediatric 18F-FDG PET/MR protocol: is administration of gadolinium chelates necessary?** *J Nucl Med* 2016;57:70–77 [CrossRef Medline](#)
- Purohit BS, Ailianou A, Dulguerov N, et al. **FDG-PET/CT pitfalls in oncological head and neck imaging.** *Insights Imaging* 2014;5:585–602 [CrossRef Medline](#)
- Gupta T, Master Z, Kannan S, et al. **Diagnostic performance of post-treatment FDG PET or FDG PET/CT imaging in head and neck cancer: a systematic review and meta-analysis.** *Eur J Nucl Med Mol Imaging* 2011;38:2083–95 [CrossRef Medline](#)
- Kim SY, Lee S, Nam SY, et al. **The feasibility of 18F-FDG PET scans 1 month after completing radiotherapy of squamous cell carcinoma of the head and neck.** *J Nucl Med* 2007;48:373–78 [Medline](#)
- Varoquaux A, Rager O, Poncet A, et al. **Detection and quantification of focal uptake in head and neck tumours: (18)F-FDG PET/MR versus PET/CT.** *Eur J Nucl Med Mol Imaging* 2014;41:462–75 [CrossRef Medline](#)
- Yamaga E, Toriihara A, Nakamura S, et al. **Clinical usefulness of 2-deoxy-2-[18F] fluoro-d-glucose-positron emission tomography/computed tomography for assessing early oral squamous cell carcinoma (cT1-2N0M0).** *Jpn J Clin Oncol* 2018;48:633–39 [CrossRef Medline](#)
- Kubiessa K, Purz S, Gawlitza M, et al. **Initial clinical results of simultaneous 18F-FDG PET/MRI in comparison to 18F-FDG PET/CT in patients with head and neck cancer.** *Eur J Nucl Med Mol Imaging* 2014;41:639–48 [CrossRef Medline](#)
- Queiroz MA, Hüllner M, Kuhn F, et al. **PET/MRI and PET/CT in follow-up of head and neck cancer patients.** *Eur J Nucl Med Mol Imaging* 2014;41:1066–75 [CrossRef Medline](#)
- Schaarschmidt BM, Gomez B, Buchbender C, et al. **Is integrated 18F-FDG PET/MRI superior to 18F-FDG PET/CT in the differentiation of incidental tracer uptake in the head and neck area?** *Diagn Interv Radiol* 2017;23:127–32 [CrossRef Medline](#)
- Becker M, Varoquaux AD, Combescure C, et al. **Local recurrence of squamous cell carcinoma of the head and neck after radio (chemo)therapy: diagnostic performance of FDG-PET/MRI with diffusion-weighted sequences.** *Eur Radiol* 2018;28:651–63 [CrossRef Medline](#)
- Queiroz MA, Wollenweber SD, von Schulthess G, et al. **Clinical image quality perception and its relation to NECR measurements in PET.** *EJNMMI Phys* 2014;1:103 [CrossRef Medline](#)
- Monti S, Cavaliere C, Covello M, et al. **An evaluation of the benefits of simultaneous acquisition on PET/MR coregistration in head/neck imaging.** *J Healthc Eng* 2017;2017:1–7 [CrossRef Medline](#)
- Boss A, Stegger L, Bisdas S, et al. **Feasibility of simultaneous PET/MR imaging in the head and upper neck area.** *Eur Radiol* 2011;21:1439–46 [CrossRef Medline](#)
- Lee SJ, Seo HJ, Cheon GJ, et al. **Usefulness of integrated PET/MRI in head and neck cancer: a preliminary study.** *Nucl Med Mol Imaging* 2014;48:98–105 [CrossRef Medline](#)
- Platzek I, Beuthien-Baumann B, Schneider M, et al. **PET/MRI in head and neck cancer: initial experience.** *Eur J Nucl Med Mol Imaging* 2013;40:6–11 [CrossRef Medline](#)
- Grueneisen J, Sawicki LM, Schaarschmidt BM, et al. **Evaluation of a fast protocol for staging lymphoma patients with integrated PET/MRI.** *PLoS One* 2016;11:e0157880 [CrossRef Medline](#)
- Todd DJ, Kay J. **Gadolinium-induced fibrosis.** *Annu Rev Med* 2016;67:273–91 [CrossRef Medline](#)
- Queiroz MA, Hüllner M, Kuhn F, et al. **Use of diffusion-weighted imaging (DWI) in PET/MRI for head and neck cancer evaluation.** *Eur J Nucl Med Mol Imaging* 2014;41:2212–21 [CrossRef Medline](#)
- Perkins NJ, Schisterman EF. **The inconsistency of “optimal” cutpoints obtained using two criteria based on the receiver operating characteristic curve.** *Am J Epidemiol* 2006;163:670–75 [CrossRef Medline](#)
- Fruehwald-Pallamar J, Czerny C, Mayerhoefer ME, et al. **Functional imaging in head and neck squamous cell carcinoma: correlation of PET/CT and diffusion-weighted imaging at 3 Tesla.** *Eur J Nucl Med Mol Imaging* 2011;38:1009–19 [CrossRef Medline](#)

32. Barakos JA, Dillon WP, Chew WM. **Orbit, skull base, and pharynx: contrast-enhanced fat suppression MR imaging.** *Radiology* 1991;179:191–98 [CrossRef Medline](#)
33. Tokuda O, Harada Y, Matsunaga N. **MRI of soft-tissue tumors: fast STIR sequence as substitute for T1-weighted fat-suppressed contrast-enhanced spin-echo sequence.** *Am J Roentgenol* 2009;193:1607–14 [CrossRef Medline](#)
34. Folkman J. **Clinical applications of research on angiogenesis.** *N Engl J Med* 1995;333:1757–63 [CrossRef Medline](#)
35. Mérida I, Avila-Flores A. **Tumor metabolism: new opportunities for cancer therapy.** *Clin Transl Oncol* 2006;8:711–16 [CrossRef Medline](#)
36. Amit M, Binenbaum Y, Trejo-Leider L, et al. **International collaborative validation of intraneural invasion as a prognostic marker in adenoid cystic carcinoma of the head and neck.** *Head Neck* 2015;37:1038–45 [CrossRef Medline](#)
37. Yousem DM, Gad K, Tufano RP. **Resectability issues with head and neck cancer.** *AJNR Am J Neuroradiol* 2006;27:2024–36 [Medline](#)
38. van den Brekel MW, Runne RW, Smeele LE, et al. **Assessment of tumour invasion into the mandible: the value of different imaging techniques.** *Eur Radiol* 1998;8:1552–57 [CrossRef Medline](#)
39. Samarin A, Hüllner M, Queiroz MA, et al. **18F-FDG-PET/MR increases diagnostic confidence in detection of bone metastases compared with 18F-FDG-PET/CT.** *Nucl Med Commun* 2015;36:1165–73 [CrossRef Medline](#)
40. Schroeder U, Dietlein M, Wittekindt C, et al. **Is there a need for positron emission tomography imaging to stage the N0 neck in T1-T2 squamous cell carcinoma of the oral cavity or oropharynx?** *Ann Otol Rhinol Laryngol* 2008;117:854–63 [CrossRef Medline](#)